Dislocation-Source Shutdown and the Plastic Behavior of Single-Crystal Micropillars

H. Tang,[1] K. W. Schwarz,[2] and H. D. Espinosa[1,*]

[1]*Department of Mechanical Engineering, Northwestern University, 2145 Sheridan Road, Evanston, Illinois 60208-3111, USA*
[2]*IBM Watson Research Center, Yorktown Heights, New York 10598, USA*

(Received 26 July 2007; published 6 May 2008)

Dislocation dynamics simulations have been used to study the stress-strain response of single-crystal micropillars containing initial dislocation networks generated via a relaxation procedure intended to approximate real thermal annealing processes. We find that, when such networks are loaded, they exhibit periods of plastic deformation, caused by the operation of single junction-stabilized spiral sources, followed by intervals of purely elastic straining when the sources shut down. The results provide insight into the mechanisms responsible for the experimentally observed staircase stress-strain behavior.

DOI: 10.1103/PhysRevLett.100.185503 PACS numbers: 62.20.F−, 61.72.Hh, 61.72.Lk

The motion of dislocations is the primary mechanism for the plastic deformation of crystalline materials [1]. The tendency of such materials to become more resistant to plastic deformation as the sample size is decreased to the micron scale has been a research topic of considerable importance for several decades [2–15]. To date, however, the dislocation behavior leading to these plasticity size effects has not been fully understood. Although the theoretical focus in the past two decades has been on the role of strain gradients and the associated geometrically necessary dislocations as the possible cause of size-dependent plastic behavior [5,6], size-dependent plasticity in the absence of loading gradients has recently been observed in submicron freestanding face center cubic (fcc) metal films [7] and in uniaxial compression experiments performed on single-crystal metallic micropillars with diameters in the micron range [2–4]. This suggests that size effects (in these cases at least) arise primarily from the dynamics of the dislocations mediating the plasticity.

A surprising feature of the compression stress-strain curves obtained from the micropillar experiments is that discrete strain bursts are separated by intervals of nearly elastic loading. According to the model proposed by Greer, Oliver, and Nix [4], the elastic loading between strain bursts strongly suggests that the micropillars become ''dislocation-starved'' following each burst. However, the details of the occurrence of strain bursts and the causes of dislocation starvation remain somewhat mysterious and can be understood only by taking a closer look at the actual dislocation behavior.

Dislocations pinned at both ends (Frank-Read sources) or, near a surface, at one end (spiral sources) can multiply via a cyclic growth and reconnection process, and it is the competition of this multiplication process against the loss of dislocations as they move to the sample surface which has been presumed to give rise to the observed behavior. In earlier computational studies [8–14] of the plastic behavior of thin films and micropillars, the initial dislocation configuration prior to loading consisted of an arbitrarily chosen set of simple Frank-Read sources. Such a model, although widely used, is actually an *ad hoc* guess at the initial dislocation structure in the micropillars and is incapable of providing insight into the origin of the sources or the details of their operation. In reality, it is known that dislocations in well-annealed crystal samples larger than a few nanometers usually take the form of a fairly regular Frank network [1]. Hence, any volume dislocation sources must be expected to develop from these networks. We thus find it essential to use such an initial state as the starting point of our investigation.

To generate a simulacrum of the initial annealed dislocation structure, we begin with a starting configuration consisting of randomly distributed straight and jogged dislocation lines [16]. Line orientation and jog size were generated randomly. Figure 1(a) shows such a structure in a micropillar having a diameter of 400 nm with the height-to-diameter ratio equal to 3. The sample contains 96 dislocation lines, half of them jogged, with an equal number assigned to each of the 12 slip systems of an fcc crystal. The material parameters for the crystal include the shear modulus $G = 42.3$ GPa, the Poisson ratio $\nu = 0.3$, and the Burgers vector magnitude $b = 0.26$ nm. As shown in the figure, all of the dislocation lines terminate on the micropillar surface. The initial dislocation structure is then allowed to evolve dynamically without external loading and is observed to gradually reorganize itself into an equilibrium configuration through both short- and long-range interactions. All calculations were carried out by using the PARANOID dislocation dynamics code [17–19]. Only dislocation glide is accounted for in the simulations conducted here. As demonstrated in Refs. [19,20], the long-range image forces resulting from traction-free boundary conditions on the surface of the micropillars give rise to relatively small corrections. These terms were therefore neglected, the approximation discussed in Ref. [19] based on Lothe's formula being used to treat the dislocation-surface interaction.

As expected, junction-forming interactions play a significant role in ensuring the formation of a stable dislocation network. Dislocation annihilations at surfaces are also

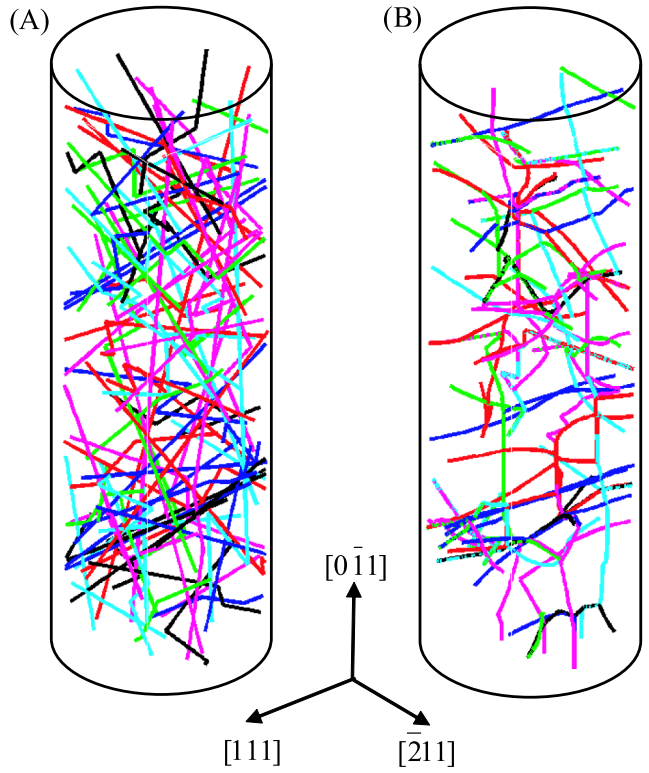

FIG. 1 (color online). Dislocation configurations in a single-crystal micropillar oriented in the [0$\bar{1}$1] direction. (a) Dislocation configuration before relaxation. (b) Dislocation network arising from full relaxation of the dislocation structure displayed in (a).

an important part of the relaxation process. Thus, the dislocation density in the fully relaxed structure is always lower than that in the initial configuration. By defining the dislocation density as the total dislocation line length divided by the volume of the pillar, the initial dislocation density for the structure shown in Fig. 1(a) is $2.9 \times 10^{14}/\mathrm{m}^2$. The dislocation density decreases to $1.89 \times 10^{14}/\mathrm{m}^2$ as the stable structure shown in Fig. 1(b) is achieved. We point out that this density is almost 2 orders of magnitude larger than the typical density for a well-annealed material in bulk ($\sim 10^{12}/\mathrm{m}^2$), a result that is not surprising given the scaling properties of dislocation dynamics.

The final dislocation configuration achieved by the relaxation process is shown in Fig. 1(b). As shown in this plot, the initially straight dislocation lines become curved, forming a network with additional jogs as well as a number of local dislocation tangles and many junctions [at least 48 junctions and different types of locks were observed in the structure shown in Fig. 1(b)]. Many potential dislocation sources occur naturally in this relaxed configuration, while at the same time neither source number nor strength is arbitrarily predefined. That is, both the number of sources and their behavior will emerge physically as the micropillar is subjected to external loading. In the present study, all pillars are oriented in the [0$\bar{1}$1] direction and subjected to uniaxial compression. We note that in this case there are a number of dislocations lying on the slip planes parallel to the loading axis. As will become obvious below, this increases the probability of dislocation-source occurrence since an unloaded dislocation arm may serve as the pole of a spiral source.

To analyze the micropillar constitutive behavior, we follow the test control methods used by Dimiduk, Uchic, and Parthasarathy [3], which result in stress-strain curves that display large strain bursts separated by nearly elastic loading. In the computations, we simulate the loading conditions used in their experiments by discretely increasing the applied stress by a small fixed value every time the plastic strain rate approaches zero. The stress-strain curves depicted in Fig. 2 were obtained by applying this procedure (using stress increments of 50 MPa) to three 400-nm-diameter pillars with different initial dislocation configurations. The initial dislocation density in all three cases is about the same. The starting configurations are displayed as insets in Fig. 2. The reader will note the strong dependence of the stress-strain response on the initial dislocation configuration. Indeed, a dislocation tangle such as that shown in Fig. 1(b) represents a nonlinear dynamical system, the behavior of which is exquisitely sensitive to initial conditions. This sensitivity was observed experimentally for submicron diameter pillars [4].

Figure 2 shows that at the beginning of the loading the response is characterized by frequent small strain bursts. This is seen in all three curves in Fig. 2. These bursts

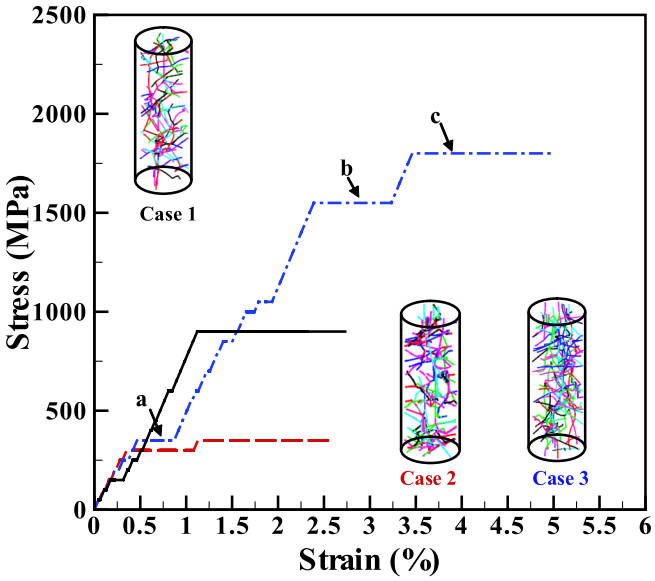

FIG. 2 (color online). Stress-strain curves corresponding to three different initial dislocation configurations in 400-nm-diameter micropillars. The initial dislocation densities are about the same for all three configurations. The sensitivity of the stress-strain responses to the initial dislocation configurations is clearly observed.

correspond to the release of individual dislocations, which then glide to the surface and are annihilated. At larger loading levels, we observe large strain bursts separated by intervals of nearly elastic loading. In the simulations, strain bursts such as those labeled (a), (b), and (c) in Fig. 2 are clearly identified as arising from the operation of single sources, almost all of which are of the generic form illustrated in Fig. 3. Here one part (OA) of a jogged dislocation line lies on the slip plane parallel to the loading axis such that it is not subject to any force arising from the pillar compression. The other part (OB) glides on a different slip plane tilted with respect to the loading axis. Under loading, this arm can rotate around the jog corner O, producing continuous plastic flow. As the arm OB rotates, however, the point O is free to move back and forth along the glide-plane intersection line CD. In the size ranges that we have studied, this motion will typically allow O to reach the surface, causing arm OB to be annihilated and consequently destroying the source. An important additional feature of the active sources that we observe is therefore the presence of a junction EF between the unloaded arm and a second dislocation. This junction dynamically limits the motion of O and thus stabilizes the source. The stability of any specific source of course depends on the exact positions of the jog corner and the junction, as well as on the strength of the loading, but it is clear that the smaller the sample diameter, the more likely it would be for the jog corner O to reach the free surface.

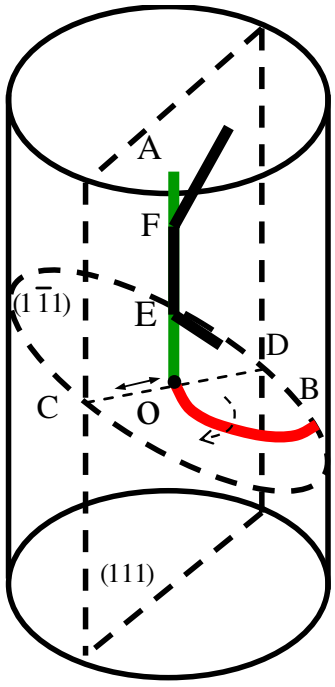

FIG. 3 (color online). Schematic diagram of a typical dislocation-source configuration. Under uniaxial compression, the dislocation line lying on the slip plane experiences the external loading and glides on the slip plane. Note that the joint node O must moves along the intersection line CD. When the joint node meets the surface, the dislocation source ceases to operate.

Although the present Letter is focused on the staircase mechanism, we note that in going from 800-nm to 200-nm samples, we also observed strong size effects not only arising from the usually assumed scaling of source-activation thresholds with sample size but also from the effect of sample size on the network dynamics, e.g., on the source shutdown mechanisms. Note that, at smaller sample dimensions, nucleation of dislocations from the sample surfaces [21], a mechanism not considered here, would need to be accounted for.

In accord with the idea that a dislocation network represents a nonlinear dynamical system, we observe that the details of the staircase behavior displayed in Fig. 2 depend somewhat on the values of applied stress increments and dislocation structures. For example, it is found that large strain bursts may appear at slightly different loading levels depending on the applied stress increment. In the simulations, a stress increment of 50 MPa was found to be computationally efficient while still being smaller than that required for the activation of the weakest source.

The activation of new sources occurs naturally as the loading is increased, but their sudden termination is perhaps more surprising. In analyzing the evolutionary behavior exhibited by the simulations, a specific mechanism can usually be associated with each source-termination event. For example, the cyclic excursions experienced by O along the glide-plane edge CD will often increase gradually as the loading increases. When O encounters the free surface, the source ceases to operate. A second frequently observed mechanism is the destruction of the junction EF constraining the motion of O. In addition, active sources were observed to be shut down by encountering a third dislocation intersecting the active glide plane. This can create a second jog or another junction deactivating the source. Such a structure can reactivate when the loading is increased further. Many of these phenomena, as well as more elaborate shutdown sequences, can be viewed in the movies provided as supplementary information [22].

It is worth pointing out that, in Ref. [14], strain burst are attributed to the destruction of jammed configurations due to long-range interactions, which produces a collective avalanchelike process. We observe that avalanches do indeed occur, not because of long-range interactions, but because the destruction of junctions can lead to the release of many dislocations. This mechanism seems to be consistent with their observations, but in our simulations it leads to only relatively small strain bursts, the released dislocations quickly escaping to the surface. The large strain bursts of primary interest are typically associated with the continuous operation of one or at most a few dislocation sources. However, the two calculations are probably not equivalent. In our simulations, plastic flow may terminate under a fixed load level due to source

shutdown. In order to generate larger plastic deformation, new sources then need to be activated at a higher load level. This essentially leads to the staircase behavior. In the simulations conducted in Ref. [14], the plastic flow can be maintained under a fixed load level because their dislocation structure consists of permanent Frank-Read sources.

In summary, we find that we are able to interpret recent experiments [2–4] on the plastic response of micropillars to zero-gradient uniaxial loading in terms of predictive dislocation dynamics. Our physical model is that the micropillars initially contain (or rapidly develop) an internal dislocation structure resembling a Frank net and that the pillar behavior reflects the response of such a structure to loading. By using three-dimensional dislocation dynamics simulations, we first generate a plausible initial Frank net structure by annealing a collection of jogged and straight dislocations under zero loads. When loaded, this structure exhibits an initial flurry of small strain bursts, evolving to a regime of large strain bursts interrupted by extended intervals of nearly elastic loading with a final stress plateau corresponding to continuous operation of a spiral source [19]. These features are in qualitative agreement with the experimentally observed behavior [2–4]. Detailed investigation shows that the large strain bursts reflect the operation of individual spiral sources consisting of a superjog, one arm of which lies on an unloaded plane, while the other arm is free to rotate on the loaded plane. Typically, these sources are stabilized by the presence of one or more junctions acting on the inactive arm. This restricts the motion of the jog corner that serves as the ''pinned'' end of the source, preventing it from reaching the free surface. Activation of such a source may be caused by the creation of a junction which stabilizes the source or by the destruction of a junction preventing the loaded arm from moving. Shutdown of such a source usually occurs when the pinned jog corner reaches the free surface. This may itself be the result of the destruction of the stabilizing junction. We point out that, in our simulations, the direction of loading was chosen to demonstrate the relevant mechanism in the clearest way, but it seems plausible that the mechanism of junction-stabilized Frank-Read sources will also play an important role for the loading directions used in the experiments of Refs. [2–4]. Further work will be required to investigate this issue.

Within the physical interpretation advanced in this work, the small sample dimensions permit only a very few sources to operate at any one time. Thus, every source activation and deactivation event has a significant effect on the plastic response. Junction creation and annihilation, and the annihilation of jog corners at the free surface, seem to be the main underlying dislocation mechanisms leading to source activation and deactivation. From the simulations, it is also inferred that stochastic variations in the initial dislocation network leads to different stress-strain signatures, a feature that is quite prevalent in pillars with submicron diameters [4]. We conclude that our interpretation, while very simple, leads naturally to the experimentally observed staircase stress-strain responses.

*espinosa@northwestern.edu

[1] J. Friedel, *Dislocations* (Pergamon, New York, 1964).
[2] M. D. Uchic, D. M. Dimiduk, T. A. Parthasarathy, J. N. Florando, and W. D. Nix, Science **305**, 986 (2004).
[3] D. M. Dimiduk, M. D. Uchic, and T. A. Parthasarathy, Acta Mater. **53**, 4065 (2005).
[4] J. R. Greer, W. C. Oliver, and W. D. Nix, Acta Mater. **53**, 1821 (2005).
[5] N. A. Fleck, G. M. Muller, M. F. Ashby, and J. W. Hutchinson, Acta Metall. Mater. **42**, 475 (1994).
[6] N. A. Fleck and J. W. Hutchinson, J. Mech. Phys. Solids **41**, 1825 (1993).
[7] H. D. Espinosa, B. C. Prorok, and B. Peng, J. Mech. Phys. Solids **52**, 667 (2004).
[8] B. von Blanckenhagen, P. Gumbsch, and E. Arzt, Model. Simul. Mater. Sci. Eng. **9**, 157 (2001).
[9] B. von Blanckenhagen, E. Arzt, and P. Gumbsch, Acta Mater. **52**, 773 (2004).
[10] H. D. Espinosa, S. Berbenni, M. Panico, and K. W. Schwarz, Proc. Natl. Acad. Sci. U.S.A. **102**, 16 933 (2005).
[11] H. D. Espinosa, M. Panico, S. Berbenni, and K. W. Schwarz, Int. J. Plast. **22**, 2091 (2006).
[12] H. Tang, K. W. Schwarz, and H. D. Espinosa, Acta Mater. **55**, 1607 (2007).
[13] Y. Xiang and J. J. Vlassak, Scr. Mater. **53**, 177 (2005).
[14] F. F. Csikor, C. Motz, D. Weygand, Z. Michael, and S. Zapperi, Science **318**, 251 (2007).
[15] T. A. Parthasarathy, S. I. Rao, D. M. Dimiduk, M. D. Uchic, and D. R. Trinkle, Scr. Mater. **56**, 313 (2007).
[16] By a jogged dislocation line, we mean a dislocation passing from one glide plane to an intersecting glide plane. Such features are created naturally by annihilation interactions between dislocations lying on intersecting glide planes.
[17] K. W. Schwarz, J. Appl. Phys. **85**, 108 (1999).
[18] K. W. Schwarz, Model. Simul. Mater. Sci. Eng. **11**, 609 (2003).
[19] X. H. Liu and K. W. Schwarz, Model. Simul. Mater. Sci. Eng. **13**, 1233 (2005).
[20] R. Gracie, G. Ventura, and T. Belytschko, Int. J. Numer. Meth. Eng. **69**, 423 (2007).
[21] B. Hyde, H. D. Espinosa, and D. Farkas, JOM **57**, 62 (2005).
[22] http://clifton.mech.northwestern.edu/~espinosa/movies/Sci-movie#.avi, # = 1, 2, 3, 4.